Soft Matter

View Online
Dynamic Article Links

Cite this: *Soft Matter*, 2011, **7**, 3744

www.rsc.org/softmatter

COMMUNICATION

Magnetic nanoparticles-induced anisotropic shrinkage of polymer emulsion droplets†

Bing Liu,*[a] Julius W. J. de Folter[b] and Helmuth Möhwald[a]

Received 9th December 2010, Accepted 22nd February 2011
DOI: 10.1039/c0sm01455a

Published on 10 March 2011 on http://pubs.rsc.org | doi:10.1039/C0SM01455A
Downloaded by Universiteit Utrecht on 05 April 2011

We here report magnetic nanoparticles (NPs)-induced buckling instability and anisotropic shrinkage behavior of polymer emulsion droplets. The oil-in-water emulsion is stabilized by the surfactant, and NPs are dispersed into the oil phase. The surface ligands (oleic acid and oleylamine) number of the NPs is an important factor to affect the shrinkage process. When a part of the ligands of the NPs is removed, the NPs show good interface attachment at the oil–water interface even with the presence of a large amount of surfactant. The increase of the interfacial viscoelasticity resulting from the attachment of NPs induced the occurrence of a buckling process. The mechanism is explored and the effect of the concentration of polystyrene and NPs is investigated in detail. The results could be helpful to understand and solve problems related with coating techniques and elastic instabilities in nature.

The drying or shrinkage of colloidal suspensions has attracted noticeable attention for fundamental and practical reasons.[1–3] Liquid droplets even only containing tiny colloidal particles show different and more complicated rheological behaviour. For example, the shell buckling phenomena was observed when a latex suspension drop was drying on the superhydrophobic planar substrate, or when a free liquid drop was shrinking on a hot plate with a temperature above 150 °C (Leidenfrost effect).[4,5] Normally, when a colloid suspension droplet is shrinking, the evaporation of the solvent results in the rise of colloidal particle concentration and the reduction of the inter-particle distance accordingly with the receding of the liquid/gas interface.[2,5,6] If the solvent loss is fast enough, these particles do not have enough time to diffuse to the bulk phase to homogenize the whole liquid drop, and they will be jammed at the interface.[2] This process can transform the interface layer from a viscous liquid state to a glass-like solid state. The further loss of solvent decreases the pressure of the inner phase. Under the external pressure, the elasticity of the shell results in an inversion of curvature. However, the onset of buckling is dependent on particle interaction.[5] Before the occurrence of buckling, the liquid droplet behavior is dominated by its viscosity, thus the shrinkage process is isotropic.[7] However, the buckling of the shell results in an anisotropic shrinkage.

Similar buckling phenomena have been intensively studied in the shrinkage of the interface of Pickering emulsion. Generally, simple liquid drops have isotropic interface shrinkage in a continuous bulk phase with the solvent evaporation.[8] However, colloidal particles are considered to irreversibly attach to an oil–water interface by a self-driving of minimum energy. This attaching behavior could affect the interface properties.[9–11] The corresponding reduction of the interfacial energy is expressed as $E = \pi r^2 \gamma_{ow}(1 + \cos\theta)^2$, where r is particle radius, γ_{ow} is the tension of the oil–water interface, and θ is the contact angle measured through the water phase.[9] Those particles with a contact angle close to 90° have the highest interface detaching energy. Therefore, once the particles are attached to an oil–water interface, the shrinkage of the interface will compress the interparticle distance. If capillary pressure overcomes the repulsive electrostatic force between particles, a stiff shell forms.[12–14] In this case, the occurrence of buckling will result in the formation of a hollow shell or capsule.[15,16] The wall consisting of colloidal particles was proven to have a reversible crumpling behavior by repeated compressing and expanding.[14]

The buckling phenomenon is also observed for the drying of aqueous polymer droplet on the substrate with different wetting properties. The difference of concentration induces different final morphology such as the so-called pancake and "Mexican hat" shape.[17,18]

When the liquid droplet is the colloid–polymer suspension, the system is more complicated since polymer could alter the particles interaction, and thus their drying behavior.[19] In electrostatic force-stabilized PS particle suspension, the addition of PEO shortens the time until buckling happens, which is more apparent for PEO with a high molecular weight.[20] However, so far, most of these investigations and studies are based on larger particles with a size above 100 nm and stable surface composition, such as polystyrene and silica particles. In the promising application of the colloidal suspension, functional metal or metal oxide NPs such as magnetic NPs, semiconductor NPs, quantum dots (QDs) have also become quite important. Therefore, investigating and understanding the shrinkage behavior of these liquid drops is highly demanded.

Herein we report the buckling phenomenon and anisotropic shrinkage based on surfactant-stabilized emulsion droplets

[a]*Department of Interfaces, Max-Planck Institute of Colloids and Interfaces, 14476 Potsdam, Germany. E-mail: liubing@iccas.ac.cn*
[b]*Van't Hoff Laboratory for Physical and Colloid Chemistry, Debye Institute for Nano-materials Science, Utrecht University, Padualaan 8, 3584 CH Utrecht, The Netherlands*

† Electronic supplementary information (ESI) available: Experimental methods, calculation, characterization of magnetic properties of NPs and the information of composite particles. See DOI: 10.1039/c0sm01455a

This journal is © The Royal Society of Chemistry 2011

View Online

Published on 10 March 2011 on http://pubs.rsc.org | doi:10.1039/C0SM01455A
Downloaded by Universiteit Utrecht on 05 April 2011

containing magnetic NPs. Especially, we found that the number of surface ligand has a crucial effect. We also investigated the other factors on the final morphology by a variety of controlled experiments and conjectured the possible mechanism. Surfactant-stabilized emulsion droplets are selected as a target system. 1 wt% of SDS aqueous solution is used as a continuous phase, and toluene (containing polystyrene (PS) and magnetic NPs) is used as a dispersion phase.

Magnetic NPs capped with oleic acid (OA) and oleylamine (OLA) were prepared based on Sun's method.[21] According to the literature, NPs were purified by washing with hexane for three times. In order to avoid particle aggregation, the hexane contains some OA and OLA.[21] The as-prepared NPs are well-dispersed in hexane. Because our solvent evaporation experiments are preformed using toluene as solvent, these NPs are redispersed into pure toluene. Dynamic light scattering (DLS) measurement indicates that their size distribution is polydispersed with an average size of 7.4 nm (Fig. 1a). TEM image shows they are well-dispersed in toluene (Fig. 1b). Based on the TEM image, statistics yield an average size of 5.5 nm (ESI†). The dispersion is transparent and stable (Fig. 1b, inset). The long alkyl chains of OA and OLA make magnetic NPs well-dispersed in an apolar solvent. However, the excess ligands (OA and OLA) in bulk phase could affect the interfacial behavior of NPs. In our experiments, we tried to remove the excess ligands by further washing with pure hexane for three times. Then they were dried by evaporating hexane. The dry powder was redispersed into pure toluene. The DLS measurement shows that 98.5% of the NPs remain dispersed and 1.5% of NPs form tiny aggregates (Fig. 1c), which suggest the loss of surface ligands of NPs. TEM image shows well-dispersed NPs (Fig. 1d), and corresponding statistical results yield an average size of 6 nm (ESI†). Though some tiny aggregates form, the whole dispersion remains transparent and stable over several weeks (Fig. 1d, inset), which suggests that not all of the ligand molecules are removed. However, the limited reduction of the ligand molecules is important to initiate an anisotropic shrinkage process. We quantitatively measured the ligand fraction of NPs by TGA (Fig. 1e). We assume that it is in a ligand-saturated state for the first kind of NPs and it is in a ligand-unsaturated state for the second NPs, the ligand number on the NPs surface can be calculated. It is estimated to be 4.9 chains per nm^2 for common NPs (CNPs) and 4.4 chains per nm^2 for ligand-deficient NPs (LDNPs) (for detailed calculation see ESI†). For LDNPs, the magnetic property is investigated and the corresponding magnetization curve is shown in Fig. S1†.

A given amount of NPs powder was dispersed into 0.5 ml toluene containing 10 w/v% of PS ($M_n = 40\,000$), and then the solution was emulsified in continuous water phase (1wt% of SDS). The emulsion was sealed. On the lid, a small hole was made with a 0.45 mm of syringe tip. The emulsion was then placed into a hot oil bath at 70 °C for 12 h. Normally, for a polymer emulsion droplet, the evaporation of the solvent results in a solid sphere (Fig. S2†). Porous sphere could be obtained by rapid solvent evaporation or porogen releasing.[22] When CNPs were added into the droplets, solvent evaporation resulted in the formation of PS/NPs composite spheres (Fig. 2a). Under the same experimental conditions, when LDNPs were used instead of CNPs, typical collapsed capsule-like composite particles were observed (Fig. 2b). Their sizes range from hundreds of nanometres to tens of micrometres, which is determined by polymer solution concentration, and emulsion preparation technique, *etc.* The particle surface is quite smooth (Fig. 2b, inset). Two kinds of NPs induce totally different shrinkage behavior under the same experimental conditions just because of different ligand number. In order to understand this process, it is necessary to explore the function of NPs in the droplets during the shrinkage process. By ultrathin cross-sectional TEM, NPs in PS matrix can be seen to be ring-like. This suggests that when the droplets are shrinking, NPs would prefer to

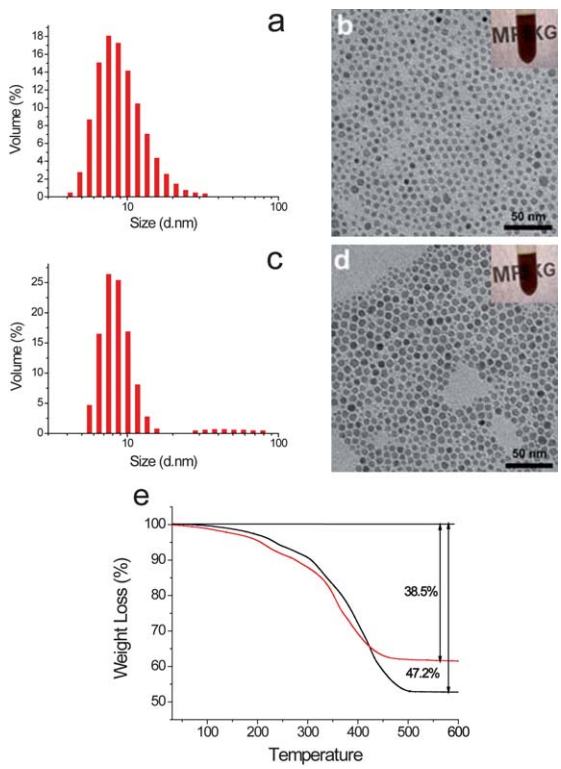

Fig. 1 Particle size distribution by DLS and corresponding TEM image (a and b) CNPs; (c and d) LDNPs; the insets show that the NPs solutions are transparent and stable; and (e) comparison of the weight loss curve of two kinds of NPs by TGA.

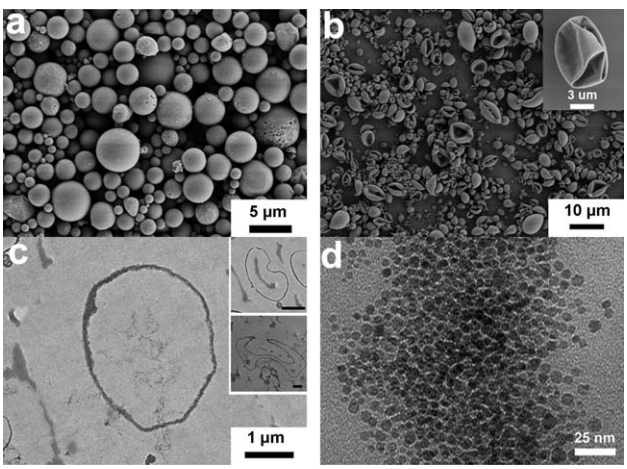

Fig. 2 SEM images of (a) PS/CNPs composite spheres and (b) collapsed PS/LDNPs composite particles ($V_{NPs}/V_{PS} = 1/17.7$); the inset is the SEM image of a single particle; (c and d) TEM images of an ultrathin cross-section of (b) with different magnifications; insets in (c) are TEM images from the same sample.

View Online

Published on 10 March 2011 on http://pubs.rsc.org | doi:10.1039/C0SM01455A
Downloaded by Universiteit Utrecht on 05 April 2011

stay at specific positions than to homogeneously disperse into the PS solution. Because almost all composite particles are collapsed, there should be no big voids inside. Hence we speculate that NPs are only in the outer part close to the PS surface. This speculation can be confirmed by the other shapes shown in Fig. 2c, inset and S3†. The TEM image with higher magnification shows these NPs consist of jammed and multilayered structures (Fig. 2d). The similar multilayered structure was reported in a Pickering emulsion polymerization of poly(DVB-MAA) particles at the interface,[23] which was explained as long-range attraction.

According to the reported liquid/gas interface shrinkage model of colloidal suspension drop, the receding of the interface results in the increase of particle concentration in the interface vicinity and slow diffusion induces a sol–gel transition of the interface.[2,4,5] This model could not totally explain our phenomena. According to the model, NPs should distribute throughout the whole PS matrix like a "coffee ring" though it is in 2D plane.[1,24] From Fig. 2c, inset (collapsed state), we did not see any NPs in the inner area. This model also could not explain that two kinds of NPs with different ligands number result in different shrinkage behaviors. Meanwhile, the droplets could not be regarded as Pickering emulsion since a large amount of surfactant was used, though similar buckling phenomena was observed.

This shrinkage process was first traced at room temperature with laser confocal scanning microscopy (LCSM). It is hard to directly image due to the movement of the liquid droplets. To weaken their movement, we added the emulsion into polyvinylalcohol (PVA, 10 wt%) aqueous solution. The picture sequence (Fig. 3) discloses the shrinkage process of single emulsion droplet. We assume that state A is the initial point (in fact, the initial point should be a little earlier because of the solvent loss within the operation time), the whole shrinkage process can be divided into two stages: (1) A to C, isotropic shrinkage stage. In this stage, the behavior of the emulsion droplet is the same with a normal liquid droplet. With the loss of the solvent, the surface area of the liquid droplet decreases, and the concentrations of NPs and PS increase gradually. At state C, sol–gel transition at the interface takes place, so state C can be considered as the onset of the buckling. According to the change of the liquid droplet diameter (Fig. 3), the loss of the solvent is around 59.6%. (2) C to D, buckling stage. In this stage, the wall buckles. Further loss of the solvent causes the wall to collapse. The final particle morphology is possibly determined by the inhomogeneity of the wall (Fig. S4†). Whether the wall collapses or not, it depends on the wall stiffness. The onset of collapse can be explained by the classical theory of thin elastic shells, which describes the critical stress (P_c) of a spherical shell as[25]

$$P_c = \frac{2}{\sqrt{3(1-\nu^2)}}\frac{Et^2}{r^2} \quad (1)$$

where t is the shell thickness, E is the Young's modulus, r is the droplet radius, and ν is the Poisson ratio. When the droplets shrink isotropically, r decreases and t increases, thus P_c increases accordingly. At state C, if P_c can resist the outer pressure, the liquid drop could remain a spherical shell. Otherwise, the wall will be in crumpling morphology.

When the surface ligand density lowers, the contact angle of NPs is closer to 90°, thus the interface detachment energy of NPs increases.[9] Therefore, ligand-deficient NPs are more likely to stay at the interface in the isotropic shrinkage stage, this promotes the sol–gel transition of the interface. However, the driving force of NPs to the interface is weakened when the interface is occupied by a large amount of surfactants. Some research groups reported that liquid droplets coalescence or particle detachment was induced when surfactant was added into Pickering emulsions or bubbles due to the adsorption of the surfactant on the particles surface.[26,27] At a high concentration of surfactant, particles were even replaced by surfactant molecules.[28] In our experiments, the surfactant concentration is high (1 wt%). In order to confirm the adsorption of NPs, we measured the static interfacial tension (γ) of water (containing 1 wt% SDS)/toluene interface by pendant drop method. The data were recorded after the adsorption equilibrium for 60 minutes. We expect that these values of γ are close to the ones which are obtained for infinite waiting time. From Fig. 4a and b, the values of γ decrease markedly with increasing NPs concentration from 0.02 to 1 w/v% without or with the presence of PS. The results suggest that it is still energy-favorable for the LDNPs to the interface. With the presence of NPs, the addition of 1 w/v% of PS results in slightly higher values of γ though the difference is small (Fig. 4b). In contrast, with the presence of 0.02 w/v% of NPs, the value of γ do not obviously decrease with increasing PS concentration from 0.2 to 1 w/v% (Fig. 4c). Pure PS do not also obviously change the value of γ with various concentration (Fig. 4d). The results suggest that NPs have a much larger effect on the interface compared with PS, and PS is not intrinsically interfacial active. Interesting is that the values of γ with PS are always higher than those without PS (Fig. 4a–c), which could originate from an interaction between NPs and PS, but further investigation is needed. However, the effect of PS and NPs to the interfacial tension is

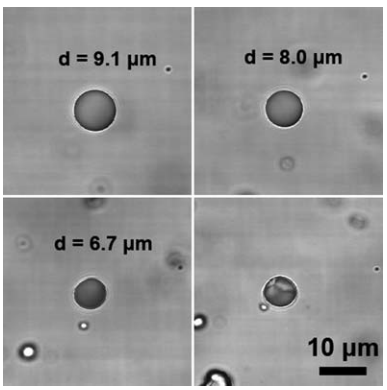

Fig. 3 LCSM image sequence showed the shrinkage process and the buckling instability of single emulsion droplet.

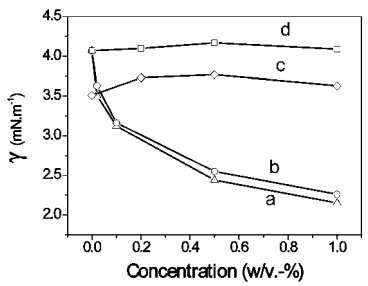

Fig. 4 Interfacial tension values (γ) of water/toluene obtained after an equilibrium for 60 min as a function of concentration of NPs or PS using a pendant drop method: (a) LDNPs; (b) LDNPs with 1 w/v% of PS; (c) PS with 0.02 w/v% of LDNPs; (d) PS. NPs and PS are in oil phase, and water means 1 wt% of SDS solution.

 This journal is © The Royal Society of Chemistry 2011

View Online

Published on 10 March 2011 on http://pubs.rsc.org | doi:10.1039/C0SM01455A
Downloaded by Universiteit Utrecht on 05 April 2011

consistent with those from dynamic interfacial tension measurements, though different apparatus result in the small difference in the obtained value of γ (Fig. S5†). The results indicate that it is the enrichment of NPs at the interface to be responsible for the formation of a stiff wall thus the buckling instability of the emulsion droplets during the process of solvent evaporation.

In order to further explore the effect of NPs on the interface, the dilational elastic modulus $E = d\gamma/d\ln A$ was measured (after 3600 s) with oscillating drop experiments performed at a frequency of 0.02 Hz (Fig. S5†). The corresponding dilational modulus (E) results are shown in Fig. 5. The absolute value of E increases with the addition of NPs. Though the measured NPs concentration is far lower than the ones used in practice, the results confirm the function of NPs to increase the stiffness of the interface. The value of E slightly decreases with the addition of PS, which could still result from an interaction between NPs and PS at the interface. We speculate that the existence of PS at the interface or in the interstice between NPs benefits the plastic deformation of the wall after the buckling happens. The position of PS in the composite particles can be confirmed by corresponding TEM images in Fig. 2, 6, 7, S3 and S6†. Therefore, for the buckling and crumpling we observed, the major reason is still the irreversible trapping of NPs in the energy well at the interface. Meanwhile, the deficiency of surface ligand could reduce the steric repulsive force between NPs thus also favour buckling. For ligand-saturated NPs, it could be that too strong hydrophobicity makes them less effectively attach to the oil–water interface for the larger effect of line tension.[29]

We also performed three groups of controlled experiments to further explore the effects of the initial concentration of NPs and polymer. In the first group of controlled experiments, PS solution was diluted so that V_{NPs}/V_{PS} is 1/2.89. The final structures show much more crumpling (Fig. 6a). A composite particle with small size is shown in Fig. 6a, inset. Different from the samples with high polymer concentration, the polymer surface is rough. Some NPs are on the surface. The TEM image shows that the NPs form a similar multilayered structure in the PS matrix as that shown in Fig. 2c (Fig. 6b). When the ratio is reduced to 1/0.74, the crumpled and coarse surface becomes more obvious (Fig. 6c). In this case, the particles are mainly consisted of NPs with 87.5 wt% content. The multilayered structure remains (Fig. 6d), though the NPs ring is possibly from the cutting of a double layered wall (Fig. 6c, inset), similar with that shown in Fig. 6b. From Fig. 6d and S6†, we can confirm that the wall mainly consisted of NPs when a high NPs ratio is used, and PS situates in the interstice between NPs. We conjecture three possible reasons for the

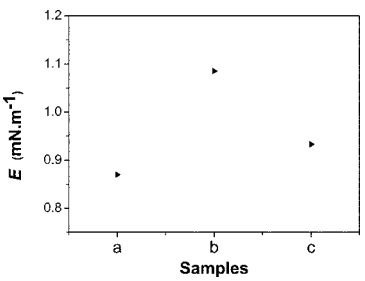

Fig. 5 Comparison of the elastic modulus of water/toluene interface: (a) toluene/water; (b) toluene (0.02 w/v% of LDNPs)/water; (c) toluene (0.02 w/v% of LDNPs + 1 w/v% of PS)/water. Water means 1 wt% of SDS solution.

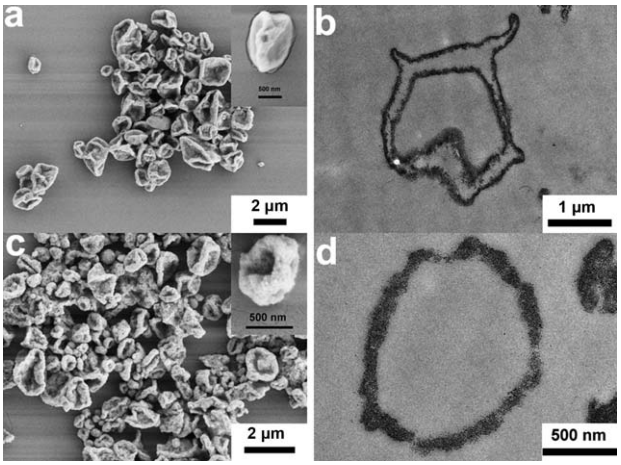

Fig. 6 SEM and TEM images (ultrathin cross-section) of two PS/NPs composite particles samples: (a and b) $V_{NPs}/V_{PS} = 1/2.89$; and (c and d) $V_{NPs}/V_{PS} = 1/0.74$.

origin of the multilayered structure: (1) when the interface is occupied by some NPs, excess NPs result in multilayered structure; (2) the shrinkage of the interface induces the re-organization of NPs in the interface vicinity; and (3) incompatibility between PS and OA/OLA stabilized NPs. We speculate that the multilayered structure favors the occurrence of the buckling by increasing the elastic modulus of the interface.

In the second group of controlled experiments, the NPs concentration is diluted so that the ratio of V_{NPs}/V_{PS} is 1/51.5. The SEM image shows the different morphology (Fig. 7a), and most of the particles maintain their spherical surface in part. The spherical part presumably is the one without NPs and exhibits only viscous

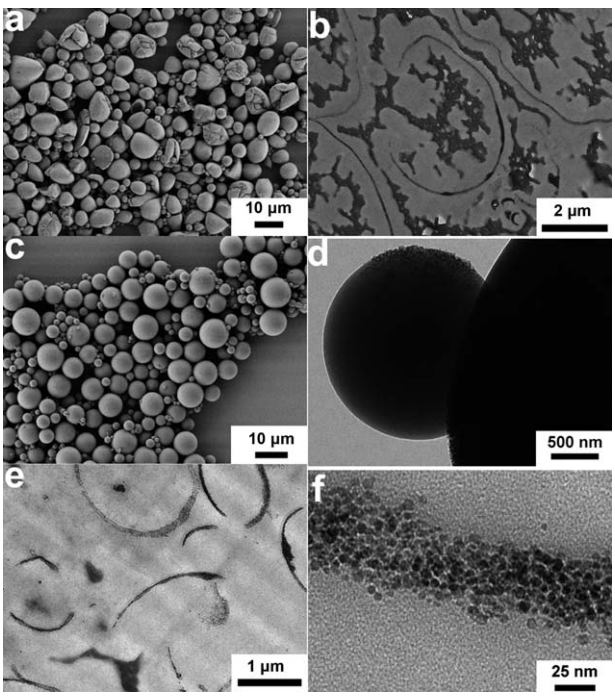

Fig. 7 SEM and TEM images of two representative PS/NPs composite particles samples: (a and b) $V_{NPs}/V_{PS} = 1/51.5$; and (c–f) $V_{NPs}/V_{PS} = 1/117$. (b) and (f) is from their ultrathin cross-section.

View Online

Published on 10 March 2011 on http://pubs.rsc.org | doi:10.1039/C0SM01455A
Downloaded by Universiteit Utrecht on 05 April 2011

shrinkage. Some evidence is shown in the TEM image where NPs form unclosed ring (Fig. 7b). From this sample, if the concentration of both NPs and PS is diluted to 10%, the final morphology is similar with those shown in Fig. 6, and NPs maintain a multilayered structure with closed ring shapes (Fig. S7†). This further illustrates that a multilayered structure is favorable for the occurrence of buckling. At the lower polymer concentration there would be enough NPs to form a multilayered structure to initiate buckling because liquid droplets can shrink to a smaller volume. Meanwhile, low polymer concentration favors the migration of NPs in polymer solution. Some small ones exhibit completely spherical shapes (Fig. S7a†), which can be attributed to the deficiency of NPs in the droplet, so that no buckling occurs (for the corresponding calculation, see ESI†). A similar result is also obtained, when the NPs amount is further reduced so that V_{NPs}/V_{PS} is 1/117. From the SEM image, no crumpled morphology is seen except for spherical shapes (Fig. 7c). The TEM image confirms in this case that NPs cover only a part of PS surface (Fig. 7d and e). Though these NPs are enough to cover the whole PS sphere, they did not form a monolayer but remain a multilayered structure (Fig. 7e and f), which could be attributed to the incompatibility between PS and OA/OLA stabilized NPs.

To exclude the influence of other parameters, we performed a third group of control experiments (Table S1†). In our system, if the anisotropic shrinkage behavior is not determined by NPs, then it must be determined by some other possibly introduced molecules. According to the synthetic process of magnetic NPs,[21] three chemicals could not be completely removed in the continuous phase. They are oleic acid, oleylamine and 1,2-hexadecanediol. However, during a similar procedure, no buckling was observed with the addition of only these molecules. This approved the function of NPs from the opposite. Moreover, after we used CTAB instead of SDS, no obvious difference was observed, so surfactant is inert. We also did the same experiments at room temperature. In principle, it renders a slower solvent evaporation. The same morphology was observed.

Similar results are observed when the direct emulsion polymerization with NPs is performed. In the first experiment, we use styrene instead of PS toluene solution, and we find that the polymerized particles obviously undergo a buckling process and anisotropic shrinkage (Fig. 8a). From the inset image, when the solidified shell resists the outer pressure or somehow the outer pressure is balanced, the hollow structure can be obtained. Because the polymerization conversion could not be 100%, some unpolymerized styrene is just "solvent" in the NPs suspension. When toluene is used to dilute the monomer styrene, a more collapsed morphology is seen (Fig. 8b), and NPs are apparently on the surface (Fig. 8b, inset).

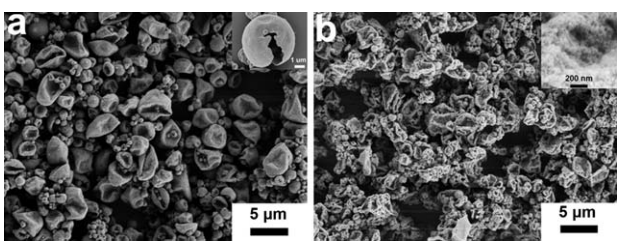

Fig. 8 SEM images of PS/NPs composite particles by direct emulsion polymerization. (A) Styrene, inset: single uncollapsed sphere; (b) styrene/toluene = 1/9, inset: the surface structure with high magnification.

In conclusion, we have explored the effect of the addition of magnetic NPs on the shrinkage behavior of surfactant stabilized polystyrene emulsion liquid droplets. To initiate an effective buckling process, the surface ligand amount of NPs is proven to be important, which could affect the interface behaviors of NPs. When a part of the ligands of NPs is removed, the NPs show good interface attachment at the oil–water interface even with the presence of a large amount of surfactant. The increase of the interfacial viscoelasticity resulted from the attachment of NPs induces an anisotropic shrinkage process of the liquid droplets. The mechanism is explored and the effect of the concentration of polymer or NPs is also investigated in detail. Some other controlled experiments are performed, which strengthened the evidence of the function of NPs during the shrinkage process. NPs form a multilayered structure at the interface, and PS situates in the interstice between NPs. When the polymer ratio is high, they also exist in the sublayer to NPs layer. The concentration of PS and NPs affects the shrinkage behavior thus different final particles morphology. A similar anisotropic shrinkage process is observed in the direct emulsion polymerization. In the forthcoming studies, the NPs with tunable wettability and different sizes will be synthesized and the corresponding interface process will be investigated in detail so as to better understand the complicated system. The understanding of this phenomenon and this process will be helpful to solve the problems related with coating techniques and understand the elastic instabilities in nature.[30]

We gratefully thank Prof. Dayang Wang for inspiring discussions, and thank Dr Antonio Stocco for measuring of interface elastic modulus and Dr Ben Erne for measuring the magnetization curve. We would like to thank Dr Jürgen Hartmann for the support on the samples characterization with electronic microscope. B. Liu was financed by the fellowship of MPI (Max-Planck Institute).

Notes and references

1 R. D. Deegan, O. Bakajin, T. F. Dupont, G. Huber, S. R. Nagel and T. A. Witten, *Nature*, 1997, **389**, 827.
2 N. Tsapis, D. Bennett, B. Jackson, D. A. Weitz and D. A. Edwards, *Proc. Natl. Acad. Sci. U. S. A.*, 2002, **72**, 12001.
3 E. Pisani, C. Ringard, V. Nicolas, E. Raphaël, V. Rosilio, L. Moine, E. Fattal and N. Tsapis, *Soft Matter*, 2009, **5**, 3054.
4 L. Pauchard and Y. Couder, *Europhys. Lett.*, 2004, **66**, 667.
5 N. Tsapis, E. R. Dufresne, S. S. Sinha, C. S. Riera, J. W. Hutchinson, L. Mahadevan and D. A. Weitz, *Phys. Rev. Lett.*, 2005, **94**, 018302.
6 P. Cicuta and D. Vella, *Phys. Rev. Lett.*, 2009, **102**, 138302.
7 D. Sen, O. Spalla, O. Taché, P. Haltebourg and A. Thill, *Langmuir*, 2007, **23**, 4296.
8 M. He, C. Sun and A. T. Chiu, *Anal. Chem.*, 2004, **76**, 1222.
9 B. P. Binks and S. O. Lumsdon, *Langmuir*, 2000, **16**, 8622.
10 K. Strarford, R. Adhikari, I. Pagonabarraga, J.-C. Desplat and M. E. Cates, *Science*, 2005, **309**, 2198.
11 A. B. Subramaniam, M. Abkarian and H. A. Stone, *Nat. Mater.*, 2005, **4**, 553.
12 J. W. Kim, A. Fernández-Nieves, N. Dan, A. S. Utada, M. Marquez and D. A. Weitz, *Nano Lett.*, 2007, **7**, 2876.
13 H. Xu, S. Melle, K. Golemanov and G. Fuller, *Langmuir*, 2005, **21**, 10016.
14 S. O. Asekomhe, R. Chang, J. H. Masliyah and J. A. W. Elliott, *Ind. Eng. Chem. Res.*, 2005, **44**, 1241.
15 I. Akartuna, E. Tervoort, A. R. Studart and L. J. Gauckler, *Langmuir*, 2009, **25**, 12419.
16 A. D. Dinsmore, M. F. Hsu, M. G. Nikoleidus, M. Marquez, A. R. Bausch and D. A. Weitz, *Science*, 2002, **298**, 1006.
17 L. Pauchard and C. Allain, *Europhys. Lett.*, 2003, **62**, 897.
18 Y. Gorand, L. Pauchard, G. Calligari, J. P. Hulin and C. Allain, *Langmuir*, 2004, **20**, 5138.

 This journal is © The Royal Society of Chemistry 2011

View Online

19 M. D. Haw, M. Gillie and W. C. K. Poon, *Langmuir*, 2002, **18**, 1626.
20 Y. Sugiyama, R. J. Larsen, J. W. Kim and D. A. Weitz, *Langmuir*, 2006, **22**, 6024.
21 S. Sun, H. Zeng, D. B. Robinson, S. Raoux, P. M. Rice, S. X. Wang and G. Li, *J. Am. Chem. Soc.*, 2004, **126**, 273.
22 G. Crotts and T. G. Park, *J. Controlled Release*, 1995, **35**, 91.
23 Z. Nie, J. I. Park, W. Li, S. A. F. Bon and E. Kumacheva, *J. Am. Chem. Soc.*, 2008, **130**, 16508.
24 D. M. Kuncicky, K. Bose, K. D. Costa and O. D. Velev, *Chem. Mater.*, 2007, **19**, 141–143.
25 A. C. Ugural, *Mechanical Design: an Integrated Approach*, McGraw Hill, New York, 2003.
26 B. P. Binks and A. Desforges, *Langmuir*, 2007, **23**, 1098.
27 A. B. Subramaniam, C. Mejean, M. Abkarian and H. A. Stone, *Langmuir*, 2006, **22**, 5986.
28 C. Vashisth, C. P. Whitby, D. Fornasiero and J. Ralston, *J. Colloid Interface Sci.*, 2010, **349**, 537.
29 R. Aveyard, B. P. Binks and J. H. Clint, *Adv. Colloid Interface Sci.*, 2003, **100–102**, 503.
30 A. J. Crosby, *Soft Matter*, 2010, **6**, 5660.

Published on 10 March 2011 on http://pubs.rsc.org | doi:10.1039/C0SM01455A
Downloaded by Universiteit Utrecht on 05 April 2011